Pyrene-Containing Conjugated Polymer-Based Fluorescent Films for Highly Sensitive and Selective Sensing of TNT in Aqueous Medium

ARTICLE *in* MACROMOLECULES · MAY 2011

Impact Factor: 5.8 · DOI: 10.1021/ma200953s

7 AUTHORS, INCLUDING:

Gang he
Chengdu University
14 PUBLICATIONS **378** CITATIONS
SEE PROFILE

Liping Ding
Shaanxi Normal University
50 PUBLICATIONS **957** CITATIONS
SEE PROFILE

Shiwei Yin
Shaanxi Normal University
88 PUBLICATIONS **2,389** CITATIONS
SEE PROFILE

Yu Fang
Shaanxi Normal University
156 PUBLICATIONS **2,562** CITATIONS
SEE PROFILE

Macromolecules

ARTICLE

pubs.acs.org/Macromolecules

Pyrene-Containing Conjugated Polymer-Based Fluorescent Films for Highly Sensitive and Selective Sensing of TNT in Aqueous Medium

Gang He, Ni Yan, Jiayu Yang, Hongyue Wang, Liping Ding, Shiwei Yin, and Yu Fang*

Key Laboratory of Applied Surface and Colloid Chemistry (Shaanxi Normal University), Ministry of Education, School of Chemistry and Materials Science, Shaanxi Normal University, Xi'an 710062, P. R. China

Supporting Information

ABSTRACT: Two poly(pyrene-*co*-phenyleneethynylene)s of different compositions (PyPE-1 and PyPE-2) were synthesized and characterized. The two polymers had been casted, separately, onto glass plate surfaces to fabricate films (film 1, film 2) for sensing performance studies. It has been demonstrated that the fluorescence emissions of the two films are sensitive to the presence of 2,4,6-trinitrotoluene (TNT) in aqueous phase. Interestingly, TNT shows little effect upon the emission of the parent polymer, poly(phenyleneethynylene) (PPE). The difference was explained by considering (1) the $\pi-\pi$ interaction between pyrene moieties contained in the copolymers and the analyte, TNT, molecules, and (2) more suitable matching of the LUMOs (lowest unoccupied molecular orbital) of the pyrene-containing conjugated polymers with that of TNT molecules. Further experiments demonstrated that the sensing is reversible and rarely encounters interference from commonly found compounds, including other nitroaromatics (NACs). Fluorescence lifetime measurements revealed that the quenching is static in nature. The smart performance of the films and the easiness of their preparation guarantee that the films may be developed into sensor devices for the supersensitive detection of TNT in groundwater or seawater.

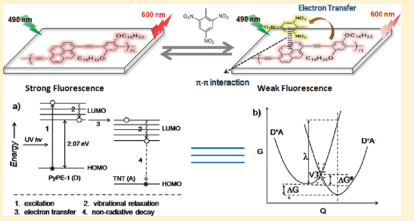

INTRODUCTION

Sensitive and selective detection of nitroaromatic compounds (NACs), particularly 2,4,6-trinitrotoluene (TNT), both in the air and in solution has attracted much attention due to security reasons.[1] Until now, chromatography,[2] surface-enhanced Raman spectroscopy,[3] amperometry,[4] energy-dispersive X-ray analysis,[5] cyclic voltammetry,[6] etc., have been employed for the detection of NACs, but these methods suffered from some of the drawbacks such as the cumbersome pretreatment of samples, interference from other compounds, low sensitivity or sophisticated instrumentation, etc.[7] In comparison, the fluorescence method possesses supersensitivity, great selectivity, low cost in instrumentation, and possibly some other advantages in the detection of NACs.[1a,b,8] For instance, Moore and co-workers[8] employed an arylene−ethynylene macrocycle as sensory material to fabricate a film sensor, which showed compelling efficiency in detection of explosive vapor due to extended 1D molecular stacking. Chen et al.[9] prepared pyrene-functionalized Ru nanoparticles as chemosensors for the sensitive detection of NACs both in the air and in organic solvents. Zhang and co-workers[10] reported a number of resonance energy-transfer-amplifying fluorescence-based chemosensors and realized sensitive and selective detection of NACs both in organic solvents and in vapor phase. Compared with low-molecular-mass fluorophores, conjugated polymers possess the so-called "molecular wire effect" or "superquenching effect", and thereby they have attracted much more attention in the exploration of sensing materials for NACs.[11] Swager and co-workers[12] developed a pentiptycene-derived PPE-based fluorescent film, of which the blue emission centering at 465 nm is supersensitive to the presence of trace amount of TNT in the air and in organic solvents. Schanze and co-workers' study[13] revealed that the thickness of a conjugated polymer film has a great effect upon its response rate to the presence of NACs in vapor phase. Pei and Liu[14] reported an electrospun nanofibrous film doped with a conjugated polymer and found that the film can be used for the detection of NACs in vapor phase with high sensitivity and selectivity. Trogler and co-workers[15] developed a new class of conjugated polymers with silicon in the main chains, and new fluorescent films were fabricated by spin-coating the polymers onto suitable solid substrates. Sensing performance studies revealed that the films are superior for detecting NACs both in the air and in organic solvents.

Sensing of NACs in groundwater or seawater is of great importance for detecting buried unexploded ordnance and for locating underwater mines.[16] There are also environmental monitoring applications for characterizing soil and groundwater contaminated by toxic TNT at military bases.[17] However, most conjugated polymer-based film sensors for explosives are applied either to the air samples or to those in organic solvents, and only a very few are used for aqueous samples. For instance, Fujiki and co-workers[18] fabricated a sensing film by casting the THF solution of fluoroalkylated polysilane onto quartz substrate. The film can be used for the detection of picric acid (PA) and DNT in aqueous phase but no significant selection to other

Received: April 26, 2011
Revised: May 14, 2011
Published: May 31, 2011

Scheme 1. Schematic Representation of the Synthesis of Conjugated Polymers PyPE-1, PyPE-2, and PPE and the Fabrication and Sensing Performance of the Films

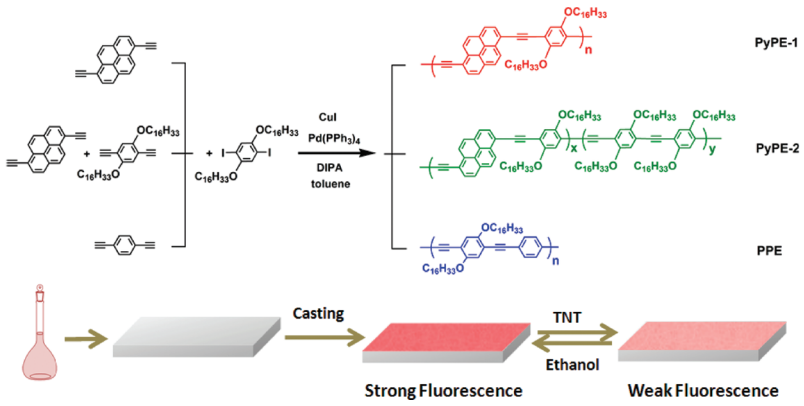

NACs. Recently, our group[19] developed several self-assembled monolayer (SAM)-based fluorescent films, which are also sensitive to the presence of NACs in air, in organic solvents, and in aqueous phase. In particular, some of the fluorescent films developed in our laboratory possess high selectivity to PA or nitrobenzene (NB).[20] To enhance selectivity, Nesterov and co-workers[21] employed cross-linked molecularly imprinted conjugated polymer (MICP) as sensing fluorophore in the creation of a TNT film sensor. However, the film as developed possesses a good selectivity to DNT rather than TNT when it is used in vapor phase. Furthermore, the response of the film to the NACs vapor is relatively slow. Sensor array was also utilized for the differentiation of different NACs of highly similar structures. Woodka and co-workers[22] reported a fluorescent sensor array which was made from five different conjugated polymers coated onto glass beads. The sensor array exhibited satisfying discrimination of different NACs when it was used in aqueous medium. A similar report was also given by Knapp and co-workers.[23] In the studies, various Zn(salicylaldimine) complexes were utilized for the buildup of a fluorescent sensor array. This array is very successful in the discrimination of different NACs even though the sensitivity is not very high. A few years ago, Anslyn and co-workers[24] employed various homogeneous fluorescence sensors for the analysis of NACs in aqueous medium. Detection of a specific NAC in the samples was realized by combinatorial analysis of the data obtained. Clearly, creation of highly selective and sensitive fluorescent films to specific NACs, particularly TNT, is a big burden to scientists working in the field, even though some progress has been made in the past few years. No doubt, there is still big room for developing novel fluorescent films with highly selectivity and sensitivity to a sepcific NAC, particularly in aqueous phase.

It is known that enlarging the effective conjugation degree of a π-system and enhancing its binding ability to an analyte is still an effective way to enhance its performance in sensing the analyte.[25] Pyrene is a well-known polycyclic aromatic compound and possesses high fluorescence quantum yield. Furthermore, it preferentially binds NACs via electron donation and acceptation interaction.[26] Accordingly, it is expected that introduction of pyrene structure into a simple but typical conjugated polymer, PPE, may bring the polymer substantial selectivity and sensitivity when it is used for the detection of NACs in aqueous phase, and thereby two poly(pyrene-*co*-phenyleneethynylene)s of different compositions were designed and synthesized (PyPE-1 and PyPE-2). On the basis of the two copolymers, film 1 and film 2 were prepared by simple casting the PyPE-1 and PyPE-2, separately, onto glass plate surfaces (Scheme 1), and their sensing performances to NACs in aqueous phase were investigated. This paper reports the details.

EXPERIMENTAL SECTION

Materials. Pyrene (Alfa, 98%), 2-methylbut-3-yn-2-ol (Alfa, 98%), trimethylsilylacetylene (Alfa, 98%), diphenylacetylene (Acros, 97%), $Pd[PPh_3]_2Cl_2$ (Alfa, 99.5%), $Pd(PPh_3)_4$ (Alfa, 99%), and CuI (Alfa, 98%) were used as received. 1,6-Diethynylpyrene, 1,4-dihexadecyloxy-2,5-diiodobenzene, and 1,4-diethynyl-2,5-dihexadecyloxybenzene were prepared by employing corresponding slightly modified literature methods.[27,28] THF and toluene were distilled from sodium benzophenone ketyl under argon prior to use. All manipulations for the preparation of the samples were performed using standard vacuum line and Schlenk techniques under a purified argon atmosphere. NACs including TNT, DNT (2,4-dinitrotoluene), NB (nitrobenzene), and PA (2,4,6-trinitrophenol) were of analytical grade and used directly without further purification. *Caution: TNT and other NACs used in the present study are highly explosive and should be handled only in small quantities.* The seawater was collected from East China Sea, located in Xiamen, China, and the seawater was used without any purification. The glass plates used in the work were commercially available microscope slides (Sail Brand, Yancheng Feizhou Bosu Co., China).

Instrumentation. The ^{1}H NMR data of the samples were collected on a Bruker AV 300 NMR spectrometer. Analysis of C, H, and N was conducted on a Perkin-Elmer 2400 CHN elemental analyzer. Fluorescence measurements were performed at room temperature on a time-correlated single photon counting Edinburgh FLS 920 fluorescence spectrometer with a front-face method. The fabricated film was inserted into a quartz cell with its surface facing the excitation light source. The cell was fixed in the solid sample holder of the instrument. The position of the film was kept constant during each set of measurements. The FTIR spectra of pressed KBr disks for the powder samples were recorded in the transparent mode using a Bruker Equinox 55 infrared spectrometer. The ellipsometric thicknesses of the layers on glass plate substrate were measured on SpecEl-2000-VIS spectroscopic ellipsometer (Mikro Pack). Gel permeation chromatography (GPC) was performed at 35 °C using THF as the eluent at a flow rate of 1.0 mL min^{-1}. The GPC instrument was equipped with a Waters 717 plus autosampler, a Waters 1515 HPLC pump, three μ-Styragel columns, and a Waters 2414 refractive index (RI) detector. The columns were

Table 1. Ellipsometric Thickness of the Fluorescent Films Fabricated on a Glass Wafer

samples	thickness ± 0.5 (nm)
PyPE-1-coated glass plate surface	18.6
PyPE-2-coated glass plate surface	19.4
PPE-coated glass plate surface	19.6

calibrated using polystyrene standards. AFM measurements were conducted on a SOLVER P47 PRO system.

Synthesis of Conjugated Polymers. *PyPE-1.* 1,4-Dihexadecyloxy-2,5-diiodobenzene (162 mg, 0.2 mmol), 1,6-diethynylpyrene (50 mg, 0.2 mmol), CuI (2 mg, 11 μmol), and $Pd(PPh_3)_4$ (12.7 mg, 11 μmol) were dissolved in a mixture of 14 mL of toluene and 6 mL of diisopropylamine. The mixture was maintained at 70 °C for 12 h, and ammonium iodide was formed immediately; the original color of the mixture is red. The mixture was filtered after cooling to room temperature, and the precipitate was washed with toluene and THF for several times. However, because of the poor solubility of PyPE-1 in the ready solvents for ^{1}H NMR and GPC, the results of ^{1}H NMR and GPC were not obtained.

PyPE-2. 1,4-Diethynyl-2,5-dihexadecyloxybenzene (61 mg, 0.1 mmol), 1,4-dihexadecyloxy-2,5-diiodobenzene (162 mg, 0.2 mmol), 1,6-diethynylpyrene (25 mg, 0.1 mmol), CuI (2 mg, 11 μmol), and $Pd(PPh_3)_4$ (12.7 mg, 11 μmol) were dissolved in a mixture of 14 mL of toluene and 6 mL of diisopropylamine. The mixture was maintained at 70 °C for 12 h, and ammonium iodide was formed immediately. The mixture is highly fluorescent, and the color of the emission turns from green to red along with the progress of the reaction, a different phenomenon from that of synthesis of PyPE-1. After cooling the mixture to room temperature, it was dropwise added into plenty of acetone (400 mL) under vigorous stirring, and precipitate was formed. The precipitate was collected and washed repeatedly with acetone, hot ethanol, and *n*-hexane and then dried overnight at 50 °C. $M_n = 1.67 \times 10^3$ by GPC (PDI = 1.4). ^{1}H NMR ($CDCl_3$) δ (ppm): 8.9−8.2 (br, 8H), 7.34−6.9 (br, 4H), 3.92 (m, 8H), 1.79−0.87 (br, 124H).

PPE. Diphenylacetylene (25 mg, 0.2 mmol), 1,4-dihexadecyloxy-2,5-diiodobenzene (162 mg, 0.2 mmol), CuI (2 mg, 11 μmol), and $Pd(PPh_3)_4$ (12.7 mg, 11 μmol) were dissolved in a mixture of 14 mL of toluene and 6 mL of diisopropylamine. The mixture was maintained at 70 °C for 12 h, and ammonium iodide was formed immediately. The mixture is highly fluorescent, and the color of the emission turns from blue to green along with the progress of the reaction. Purification of the polymer was similar to that of PyPE-2. $M_n = 1.62 \times 10^3$ by GPC (PDI = 1.63). ^{1}H NMR ($CDCl_3$) δ (ppm): 7.54 (br, 4H), 7.34 (d, 2H), 7.02−7.00 (m, 2H), 3.92 (m, 4H), 1.79 (br, 4H), 1.49 (br, 4H), 1.26 (br, 48H), 0.88 (t, 6H).

Fabrications of Conjugated Polymer-Based Fluorescent Films. A glass plate has been specifically selected as substrate due to both its cheapness and inertness to the fluorescence emission of the polymers. Before further treatment, a glass plate (0.9 cm × 2.5 cm) was cleaned in a "piranha solution" (7/3, v/v, 30% H_2O_2/98% H_2SO_4)[29] (*warning: piranha solution should be handled with extreme caution since it can react violently with organic matter*) at 98 °C for 1 h, then rinsed thoroughly with plenty of water, and finally dried at 100 °C in a dust-free oven for 1 h. The target films were prepared by casting each of the THF solutions of PyPE-1, PyPE-2, and PPE on a pretreated glass plate surface. The films as prepared are named as film 1, film 2, and film 3, respectively. The synthesis of conjugated polymers, PyPE-1, PyPE-2, and PPE, and the fabrication processes are shown in Scheme 1.

RESULTS AND DISCUSSION

Ellipsometry and Atomic Force Microscopy (AFM) Measurement. Ellipsometry is a widely used optical technique for measuring the thickness of thin organic films. In this study, the measurements of the layers were made on glass plate by assuming a refractive index of 1.5 for the layer over the substrate surface. Average values for the adlayers from the measurements are summarized in Table 1. It is seen that the thicknesses of film 1, film 2, and film 3, which was taken as a control and the polymer on it is PPE, are 18.6, 19.4, and 19.6 nm, respectively. AFM imaging revealed that the pyrene-containing copolymer aggregated into ball-like structure rather than densely packed continuous film on the substrate surface (cf. Figure S1), and furthermore, the thickness of the film is less than 1 μm, which is definitely favorable for sensing.

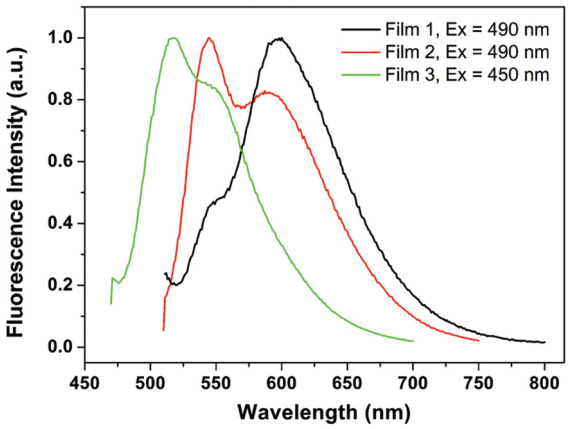

Figure 1. Emission spectra (normalized) of film 1, film 2, and film 3 in aqueous phase.

Steady-State Excitation and Emission Measurements. The excitation and emission spectra of film 1, film 2, and film 3 in aqueous medium are shown in Figure 1 and Figure S2. Comparing the profiles of the excitation spectra of the three films, it is clearly seen that the red edges of the copolymer-based films (film 1 and film 2) are significantly red-shifted if compared to that of the control film, film 3, a strong evidence to support that introduction of pyrene into the conjugated polymer chain does enhance conjugation and thereby decreases energy gap between the excited state and ground state of the parent polymer, PPE. Furthermore, the profiles of the three excitation spectra are also different from each other, especially the one of film 1 which is composed of two parts, another evidence for the existence of pyrene unit in the copolymer chain. As expected, incorporation of pyrene structure into the conjugated polymer makes its emission significantly red-shifted (cf. Figure 1). It is to be noted that the more the ratio of pyrene unit in the copolymer, the more the shift, as demonstrated by the fact that the emission of film 1 is more red-shifted in comparison with that of film 2. A similar finding has also been reported by other groups.[30] As a reference, the excitation and emission spectra of film 1 in air are displayed in Figure S3.

Stability of the Fluorescent Films. All the three films showed good photochemical stability both in aqueous phase and in air at room temperature as demonstrated by the fact that both the intensities and the profiles of the emissions barely changed after several hours scanning (cf. Figure S4). Furthermore, the films are free of leaking even if they are kept in aqueous phase for more than 1 week, which is a necessity for their analytical uses in aqueous medium. However, only film 1 can be kept in THF, toluene, and some other polar organic solvents due to its poor

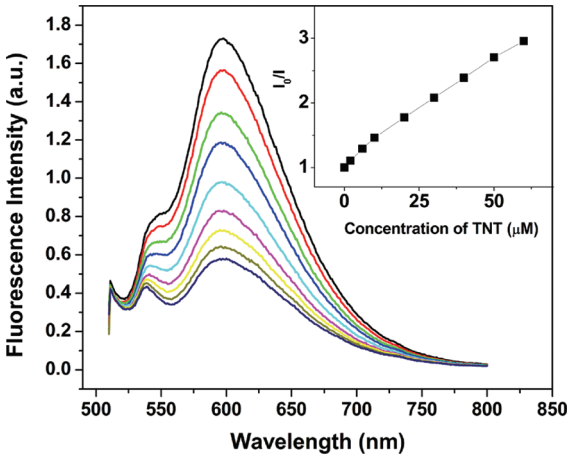

Figure 2. Fluorescence emission spectra of film 1 in the presence of different concentrations of TNT (from top to bottom: 0, 2, 6, 10, 20, 30, 40, 50, and 60 μM) in an aqueous medium (λ_{ex} = 497 nm).

solubility in them. Because of this extraordinary property, film 1 may be used in many complex mediums. From this point of view, the sensing performance of film 1 to NACs is need to be systematically studied.

Fluorescence Quenching Studies with NACs in Aqueous Medium. As expected, the fluorescence emission of Film 1 is sensitive to the presence of electron-deficient NACs, particularly TNT. Figure 2 depicts the fluorescence emission spectra of the film at various TNT concentrations in aqueous phase. It can be seen that nearly 70% of the emission is quenched when TNT reaches 60 μmol/L.

The Stern−Volmer equation was used to evaluate the differences in quenching for various analytes, where I_0 and I are the fluorescence intensities of the film in the absence and presence of NACs, respectively, [Q] is the concentration of the NACs, and K_{sv} is the Stern−Volmer constant.[31] A linear Stern−Volmer relationship was obtained in all the cases with highest quenching constant (K_{sv} = 3.26 × 10^4 M^{-1}) for TNT.

$$\frac{I_0}{I} - 1 = K_{sv}[Q] \qquad (1)$$

Similarly, film 2 is also sensitive to TNT in aqueous phase, and the corresponding K_{sv} is 3.65 × 10^4 M^{-1}, very close to that of film 1. The Stern−Volmer plots of the three films to TNT are presented in Figure 3. Clearly, the presence of TNT has little effect upon the fluorescence emission of the control film, film 3, of which the K_{sv} value is only 7.75 × 10^3 M^{-1}, significantly lower than those for the two films with pyrene-containing copolymers as sensing materials, indicating pyrene unit has played a great role for the sensitive sensing of TNT (cf. Figure 3). The highly efficient quenching of TNT to the fluorescence emissions of the copolymers can be attributed to $\pi-\pi$ interaction between the quencher, TNT, and the pyrene moieties in the copolymers and the match of their electronic structures. It is known that pyrene possesses a conjugated plane structure, which makes it easier to bind TNT via $\pi-\pi$ interaction. In principle, the quenching process could be considered as photoinduced electron transfer. The photoinduced electron (white ball shown in Figure 4) on LUMO of donor (PPE or PyPE) transfers to its neighboring electron acceptor (such as TNT). Then the electron on the LUMO of an acceptor should recombine with the donor's

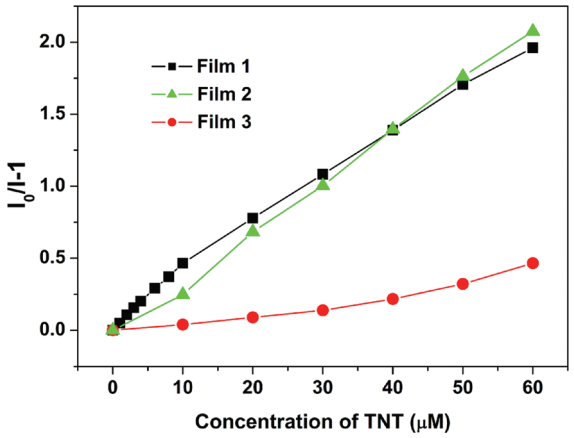

Figure 3. Stern−Volmer plots: ■ (film 1), ▲ (film 2), and ● (film 3) for TNT at different concentrations.

HOMO electron via a nonradiative process. Obviously, the quenching efficiency is directly proportional to the rate of the electron transfer. In the semiclassical limit of Marcus theory, the transfer rate is expressed as[32]

$$K_{et} = A\exp(-\Delta G^{\#}/kT) = \frac{2\pi^{3/2}}{h\sqrt{\lambda kT}} V^2 \exp\left[\frac{-(\Delta G^0 + \lambda)^2}{4\lambda kT}\right] \qquad (2)$$

where ΔG^0 means the standard Gibbs free energy difference of the electron transfer reaction, V is the electron coupling between the initial state (D^*A) and final state (D^+A^-), and λ is the reorganization energy which includes two contributions: (i) the internal part λ_i related to the geometry changes of the D and the A and (ii) the external part λ_e related to the polarizations of the surrounding medium. Under the one-electron approximation, the ΔG^0 can be estimated by the energy gap between the LUMO of the A and that of the D, which can be readily calculated by using a quantum-chemical calculation method. And electron coupling (V) can be considered as direct LUMOs coupling between the D and the A, which is strongly dependent upon the distance between them and also on the relative orientation of them. Form eq 2, we can readily note that electron-transfer rate reaches maximum when $-\Delta G^0$ is equal to λ. When $|\Delta G^0| < \lambda$, the so-called normal region, the more negative the driving force, the faster the electron transfer rate. When $|\Delta G^0| > \lambda$, the inverted region, the more negative the driving force, the slower the electron transfer rate.

The quantum-chemical methods at the B3LYP/6-31G(d)[33] level of theory using Gaussian 09[34] were employed for the calculation of the HOMO and LUMO energies for optimized geometries of the donors, including pyrene, PPE, and PyPE, and the acceptors, including TNT, DNT, and NB (Figure S5). The band gap energies are illustrated in Figure 5. It is clearly seen that introduction of pyrene structure into PPE chain lowers its frontier's band gap. It can be also noted that the LUMO energies of PPE (−2.42 eV) and PyPE (−2.44 eV) are very close, which means that the driving forces (ΔG^0) of the conjugated polymer (PPE) and its modified form (PyPE) to same analyte must be similar. Following Cornil's calculation procedure,[35] the internal reorganization energy (λ_i) was also calculated. For the systems of OPE2 + TNT and Py + TNT, the λ_i values of them are 0.230

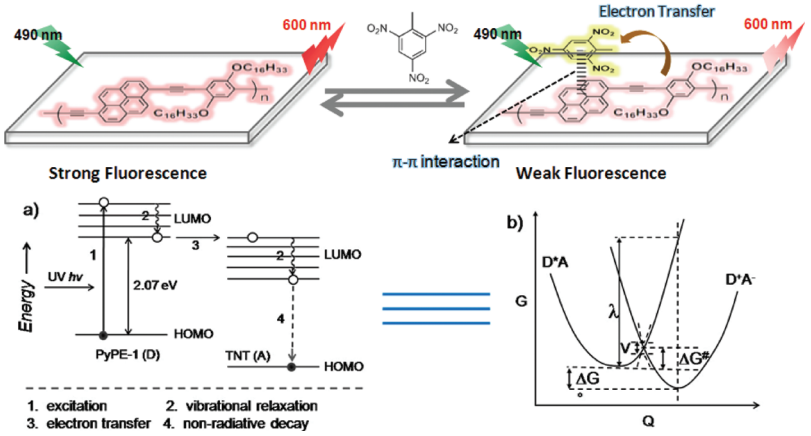

Figure 4. Schematic representation of the electron-transfer mechanism for the quenching of the fluorescence of film 1 by TNT. (a) Schematic representation of the photoinduced electron-transfer mechanism for the quenching of the fluorescence. (b) Plot of free energy versus reaction coordinates Q for reactants (D^*A) and products (D^+A^-), where ΔG^0 means the difference of the standard free energy, λ the reorganization energy, and ΔG^0 the activation energies of the electron-transfer reaction.

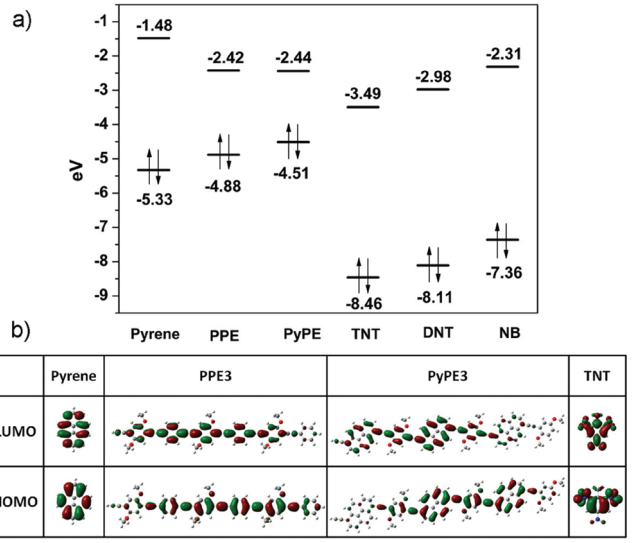

Figure 5. Frontier orbital energy correlation diagram for pyrene, PPE, and PyPE and some explosive analytes. Bottom lines represent the HOMO energies, and top lines represent the LUMO energies (a). The calculated molecular structures and lowest unoccupied molecular orbital (LUMO) of pyrene, PPE3, PyPE3, and TNT (b).

and 0.226 eV, respectively. The values are very close to the value for the system of perylenebismide and phthalocyanine, which is an idea $\pi-\pi$ stacking-based D−A system. Therefore, it was anticipated that the systems of PPE−TNT and PyPE−TNT should possess similar internal reorganization energies. But for external part, it should not be neglected because solvation is a key factor to affect the LUMO energies of the compounds particularly when the compounds are in their excited states. Therefore, the polarization of solvent was calculated by employing the generalized Born method, which can be expressed as

$$\lambda_e = (\Delta e)^2 \left[\frac{1}{\varepsilon_{opt}} - \frac{1}{\varepsilon_s}\right]\left[\frac{1}{R_D} + \frac{1}{R_A} - \frac{1}{R}\right] \qquad (3)$$

where ε_{opt} and ε_s are the optical and static dielectric constants of the solvent, respectively. R_D and R_A stand for the molecular radii of D and A, respectively, which are related to the sizes of the molecules. R is the center-to-center distance between D and A. For our PPE and PyPE coupled with TNT systems, D is a conjugated polymer with a large size which means electron transfer should not produce significant polarization. Thus, the external contribution is mainly from the solvent polarization around the analyte, TNT molecules. For these reasons, the total reorganization energies for PPE and PyPE coupled with same explosive molecules should be very close to each other. In short, from the analysis of driving forces (ΔG^0) and reorganization energies for PPE and PyPE coupled with TNT, a conclusion that the exponential terms of the two systems in eq 2 must be very similar may be drawn. Thus, the higher sensitivity of PyPE to TNT than PPE to TNT can be attributed to the electron coupling V term. It is well-known that the electron coupling term is strongly dependent on the strength of D−A interaction, which means the close contact of the D and the A molecules is a necessity for the effective interaction of the two kinds of molecules. Accordingly, in thin films the A, that is the explosive, molecules must diffuse into the π-conjugated polymer layer and form effective $\pi-\pi$ stacking-based D−A aggregates, and only in this way the electron coupling term becomes significant. Introducing pyrene structure into PPE definitely increases the disorder of the polymer layer and thereby favors the diffusion of the acceptor molecules within the layer and formation of the D−A aggregates. This may explains why PyPE-based film is more sensitive to the presence of TNT than its parent polymer, PPE.

Interestingly, the film shows not only great sensitivity but also high selectivity to TNT in aqueous phase. Figure 6 shows the Stern−Volmer plots of film 1 for each of the NACs tested. The Stern−Volmer quenching constants of the film to DNT, NB, and PA are 3.62×10^3, 1.34×10^3, and 0.45×10^3 M^{-1}, respectively, which is at least 1 order of magnitude lower than that for TNT, a clear signature to show that the film is highly selective to TNT rather than to other NACs.[36] This result may be rationalized by considering the differences of the reduction potentials of the NACs. It is known that the reduction potentials of TNT, DNT, and NB in aqueous phase are −0.7, −0.9, and −1.15 V (versus normal hydrogen electrode (NHE)), respectively.[17] Matching of the LUMO energy of TNT to the excited polymer might be the reason explaining the superior quenching process. As for PA, it is

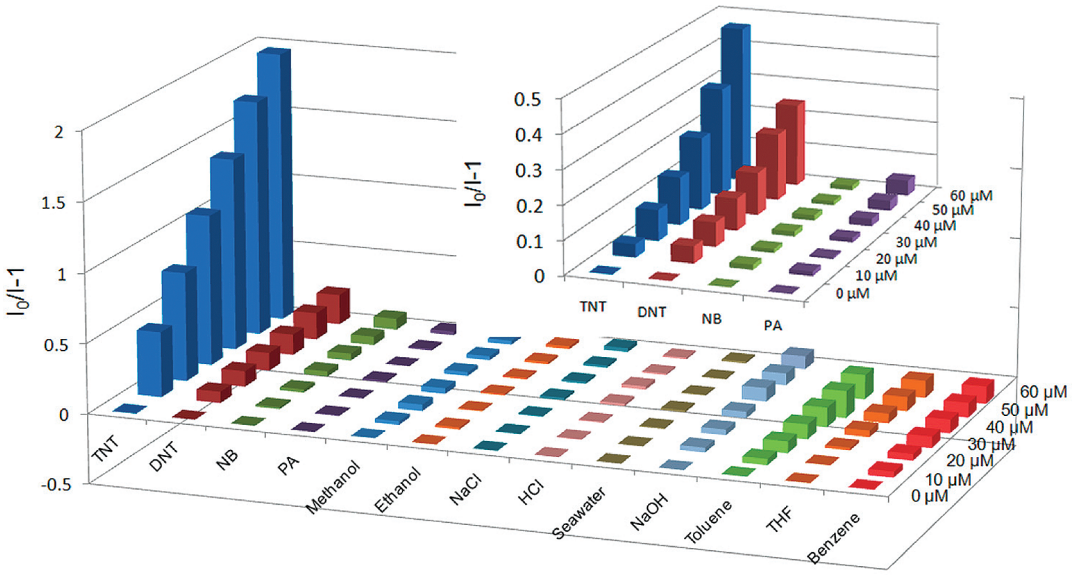

Figure 6. Stern−Volmer plots of NACs and common interferents to the fluorescence emission of film 1 at different concentrations. The inset shows the Stern−Volmer plots of NACs to the fluorescence emission of film 3 at different concentrations.

well-known that PA behaves as a relatively strong acid because of the three nitro groups affixed on the benzene ring, which makes it hydrophilic.[20b] Accordingly, the compatibility of the hydrophobic film (film 1) to PA should be poor, resulting in lower quenching efficiency. But a control experiment with film 3, of which PPE was used as a sensing polymer, demonstrated a similar sensitivity order to the analytes, but much lower selectivity to TNT (inset of Figure 6). In other words, introduction of pyrene mioety into PPE chain increased not only the sensitivity but also the selectivity of the PPE-based film to TNT. The high sensitivity and selectivity of film 1 to TNT can be described by the cartoon as shown in Figure 4.

Interference from Commonly Found Chemicals. Selectivity is a crucial criterion for the practical uses of a sensing film, and thereby it is of interest to study the response of the film to commonly found chemicals that may affect the detection of TNT in aqueous phase. The results are also shown in Figure 6. With reference to the figure, it is seen that the fluorescence emission of film 1 is rarely affected by the presence of each of the commonly found chemicals as tested. However, with a close inspection of the figure, it can be found that DNT and NaOH show positive, but limited, interference to TNT sensing. In contrast, THF, toluene, and benzene demonstrate negative, also limited, interference to the test. It is interesting to note that other chemicals including inorganic salts, seawater, PA, NB, acid, and alkali, etc., show little effect upon the test. The slight sensitization of toluene, THF, and benzene to the fluorescence emission of the film may be attributed to the so-called swelling-induced emission enhancement (SIEE) effect, which was proposed by Kwak and co-workers in the studies of the response of substituted polyacetylene film to organic solvents.[37] No interference from seawater implies that the film may be potentially usable for TNT detection in seawater.

Detection of TNT in Seawater. Figure 7 depicts the comparison of the quenching efficiencies of TNT to the fluorescence emission of film 1 in pure water and in seawater. It is clearly seen, as expected, that the two Stern−Volmer plots are nearly overlapped. In other words, this film may be a good candidate for developing into a TNT sensor for its detection in seawater.

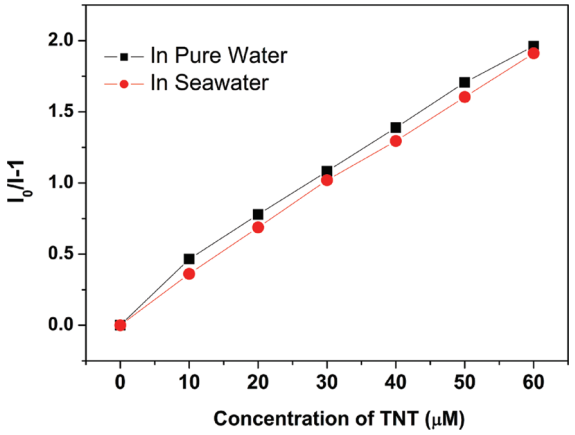

Figure 7. Stern−Volmer plots of film 1 against the concentrations of TNT in pure water (■) and in seawater (●).

Quenching Mechanism of the Sensing Process. It is well-known that fluorescence quenching can be divided into static quenching and dynamic quenching. The natures of the two quenching processes are very different. For static quenching, formation of a nonfluorescent fluorophore−quencher complex is the origin of the quenching. For dynamic quenching, however, collision of the molecules of a quencher to the excited molecules of the fluorophore under study is a necessity, and thereby dynamic quenching is a diffusion-controlled process. Clearly, static quenching does not affect the fluorescence lifetime of the fluorophore under study. In contrast, dynamic quenching must reduce the lifetime. Therefore, comparison of the dependence of fluorescence intensity to the concentration of a quencher with the dependence of fluorescence lifetime to the concentration can reveal the quenching nature. On the basis of these considerations, both fluorescence intensity and fluorescence lifetime were measured as functions of TNT concentration. The results are shown in Figure 8. It is obvious that the fluorescence lifetime of the film is almost invariable along with the increase of the TNT concentration, indicating that the quenching is static in nature, in

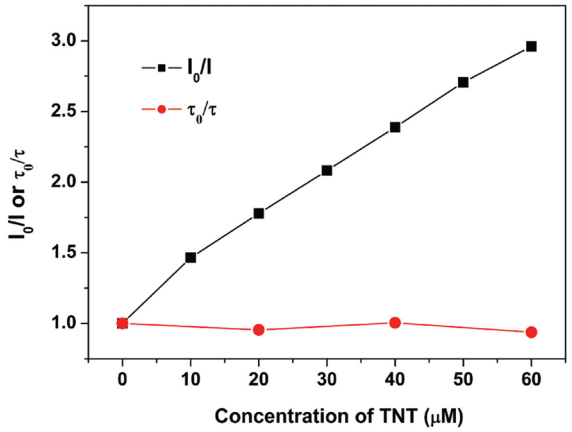

Figure 8. Plots of the ratios of I_0/I and τ_0/τ of film 1 against the concentration of TNT.

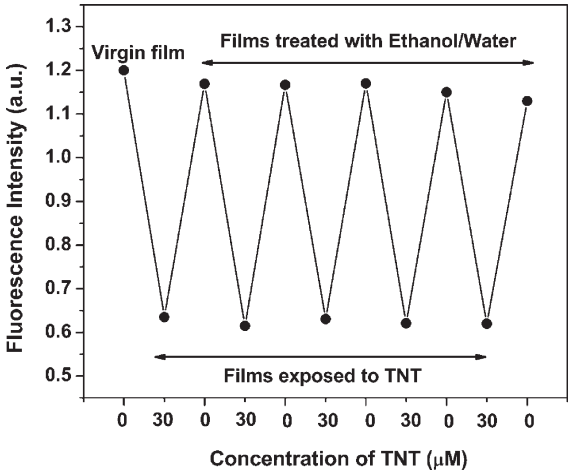

Figure 9. Reversibility of the response of film 1 to TNT.

support of the assumption that the conjugated copolymer possesses specific affinity to TNT and forms a nonfluorescent complex with the quencher, TNT. Another necessity for a usable sensing film is its reversibility. In other words, the film can be usable in real-life applications only when the sensing process is reversible. Accordingly, the reversibility of the sensing process was also examined.

Reversibility of the Quenching Process. The procedures adopted for the examination of the reversibility of the sensing process are as follows: first, the film was inserted into a cell with 2.5 mL of distilled water, and the fluorescence emission of the film was recorded. Second, 30 μL of TNT solution (0.0025 mol/L) was added, and after 10 min equilibration the fluorescence emission of the film was recorded again. Third, after the measurement, the film was taken out of the cell, immersed in ethanol for 30 min, and then washed with distilled water for several times. The film was reused after the treatment, and the whole process was repeated for several times. The results are shown in Figure 9. Reference to the figure, it is clear that the response of film 1 to TNT is fully reversible. Furthermore, the film is stable for 6 months at least provided it is properly preserved.

CONCLUSION

Pyrene as a commonly found superior low-molecular-mass fluorophore was purposely and successfully introduced into a simple but typical conjugated polymer, PPE, and two pyrene-containing conjugated copolymers, PyPE-1 and PyPE-2, which possess different compositions, were synthesized. The two copolymers and a control polymer, PPE, were casted respectively onto glass plate surfaces to fabricate fluorescent films (film 1, film 2, and film 3). Fluorescence studies revealed that film 1 and film 2 are very sensitive to the presence of TNT in aqueous medium. Commonly found interferents including DNT, NB, and PA show little interference to the fluorescence emission of the films. The great quenching effect of TNT to the emission of the copolymers have been attributed to the selective binding of the copolymers to the quencher via specific $\pi-\pi$ interaction and the match of the LUMO of the copolymers to that of the quencher. Further experiments demonstrated the reversibility and the static nature of the sensing process. Interestingly, film 1 can be used for TNT sensing in seawater or groundwater, indicating that the film may find real-life applications.

ASSOCIATED CONTENT

Supporting Information. Details of AFM, excitation spectra, stability of the fluorescent films, calculation of band gap energies, and quenching efficiencies of TNT and DNT to the fluorescence emission of film 1. This material is available free of charge via the Internet at http://pubs.acs.org.

AUTHOR INFORMATION

Corresponding Author

*E-mail: yfang@snnu.edu.cn. Tel: 0086-29-85300081. Fax: 0086-29-85307566.

ACKNOWLEDGMENT

The authors thank the Natural Science Foundation of China (Nos. 20803046 and 20927001), the Ministry of Science and Technology of China (No. 2007AA03Z349), and the 13115 program of Shaanxi Province (No. 2010ZDKG-89) for financial support.

REFERENCES

(1) (a) McQuade, D. T.; Pullen, A. E.; Swager, T. M. *Chem. Rev.* **2000**, *100*, 2537–2574. (b) Albert, K. J.; Lewis, N. S.; Schauer, C. L.; Sotzing, G. A.; Stitzel, S. E.; Vaid, T. P.; Walt, D. R. *Chem. Rev.* **2000**, *100*, 2595–2626. (c) Toal, S. J.; Trogler, W. C. *J. Mater. Chem.* **2006**, *16*, 2871–2883. (d) Yinon, J. *Trends Anal. Chem.* **2002**, *21*, 292–301. (e) Tenhaeff, W. E.; McIntosh, L. D.; Gleason, K. K. *Adv. Funct. Mater.* **2010**, *20*, 1144–1151. (f) Filanovsky, B.; Markovsky, B.; Bourenko, T.; Perkas, N.; Persky, R.; Gedanken, A.; Aurbach, D. *Adv. Funct. Mater.* **2007**, *17*, 1487–1492.

(2) Weisberg, C. A.; Ellickson, M. L. *Am. Lab.* **1998**, *30*, 32N–32V.

(3) Sylvia, J. M.; Janni, J. A.; Klein, J. D.; Spencer, K. M. *Anal. Chem.* **2000**, *72*, 5834–5840.

(4) Hilmi, A.; Luong, J. H. T. *Anal. Chem.* **2000**, *72*, 4677–4682.

(5) Luggar, R. D.; Farquharson, M. J.; Horrocks, J. A.; Lacey, R. J. *X-Ray Spectrom.* **1998**, *27*, 87–94.

(6) Krausa, M.; Schorb, K. *J. Electroanal. Chem.* **1999**, *461*, 10–13.

(7) (a) Bruschini, C. *Subsurf. Sens. Technol. Appl.* **2001**, *2*, 301–338. (b) Moore, D. S. *Rev. Sci. Instrum.* **2004**, *75*, 2499–2512.

(8) Naddo, T.; Che, Y.; Zhang, W.; Balakrishnan, K.; Yang, X. M.; Yen, M.; Zhao, J. C.; Moore, J. S.; Zang, L. *J. Am. Chem. Soc.* **2007**, *129*, 6978–6979.

(9) Chen, W.; Zuckerman, N. B.; Konopelski, J. P.; Chen, S. *Anal. Chem.* **2010**, *82*, 461–465.

(10) Tu, R. Y.; Liu, B. H.; Wang, Z. Y.; Gao, D. M.; Wang, F.; Fang, Q. L.; Zhang, Z. P. *Anal. Chem.* **2008**, *80*, 3458–3465.
(11) (a) Swager, T. M. *Acc. Chem. Res.* **1998**, *31*, 201–207. (b) Kim, Y.; Whitten, J. E.; Swager, T. M. *J. Am. Chem. Soc.* **2005**, *127*, 12122–12130. (c) Yang, Y.; Turnbull, G. A.; Samuel, I. D. W. *Adv. Funct. Mater.* **2010**, *20*, 2093–2097.
(12) (a) Yang, J.-S.; Swager, T. M. *J. Am. Chem. Soc.* **1998**, *120*, 11864–11873. (b) Zhou, Q.; Swager, T. M. *J. Am. Chem. Soc.* **1995**, *117*, 7017–7018. (c) Zhao, D. H.; Swager, T. M. *Macromolecules* **2005**, *38*, 9377–9384.
(13) Liu, Y.; Mills, R. C.; Boncella, J. M.; Schanze, K. S. *Langmuir* **2001**, *17*, 7452–7455.
(14) Long, Y. Y.; Chen, H. B.; Yang, Y.; Wang, H. M.; Yang, Y. F.; Li, N.; Li, K. A.; Pei, J.; Liu, F. *Macromolecules* **2009**, *42*, 6501–6509.
(15) (a) Sohn, H.; Sailor, M. J.; Magde, D.; Trogler, W. C. *J. Am. Chem. Soc.* **2003**, *125*, 3821–3830. (b) Sanchez, J. C.; Urbas, S. A.; Toal, S. J.; DiPasquale, A. G.; Rheingold, A. L.; Trogler, W. C. *Macromolecules* **2008**, *41*, 1237–1245. (c) Sanchez, J. C.; Trogler, W. C. *J. Mater. Chem.* **2008**, *18*, 3143–3156. (d) Sanchez, J. C.; DiPasquale, A. G.; Rheingold, A. L.; Trogler, W. C. *Chem. Mater.* **2007**, *19*, 6459–6470.
(16) (a) Toal, S. J.; Magde, D.; Trogler, W. C. *Chem. Commun.* **2005**, 5465–5467. (b) Shriver-Lake, L.; Donner, B.; Ligler, F. *Environ. Sci. Technol.* **1997**, *31*, 837–841.
(17) Sohn, H.; Calhoun, R. M.; Sailor, M. J.; Trogler, W. C. *Angew. Chem., Int. Ed.* **2001**, *40*, 2104–2015.
(18) Saxena, A.; Fujiki, M.; Rai, R.; Kwak, G. *Chem. Mater.* **2005**, *17*, 2181–2185.
(19) Ding, L. P.; Fang, Y. *Chem. Soc. Rev.* **2010**, *39*, 4258–4273.
(20) (a) Zhang, Y.; He, G.; Liu, T.; Yang, M.; Ding, L.; Fang, Y. *Sensor Lett.* **2009**, *7*, 1141–1146. (b) He, G.; Peng, H. N.; Liu, T. H.; Yang, M. N.; Zhang, Y.; Fang, Y. *J. Mater. Chem.* **2009**, *19*, 7347–7353.
(21) Li, J. H.; Kendig, C. E.; Nesterov, E. E. *J. Am. Chem. Soc.* **2007**, *129*, 15911–15918.
(22) Woodka, M. D.; Schnee, V. P.; Polcha, M. P. *Anal. Chem.* **2010**, *82*, 9917–9924.
(23) Germain, M. E.; Knapp, M. J. *J. Am. Chem. Soc.* **2008**, *130*, 5422–5423.
(24) Hughes, A. D.; Glenn, I. C.; Patrick, A. D.; Ellington, A.; Anslyn, E. V. *Chem.—Eur. J.* **2008**, *14*, 1822–1827.
(25) (a) Bai, H.; Li, C.; Shi, G. Q. *Sens. Actuators, B* **2008**, *130*, 777–782. (b) Venkataramana, G.; Sankararaman, S. *Org. Lett.* **2006**, *8*, 2739–2742. (c) Shimizu, H.; Fujimoto, K.; Furusyo, M.; Maeda, H.; Nanai, Y.; Mizuno, K.; Inouye, M. *J. Org. Chem.* **2007**, *72*, 1530–1533.
(26) Zhang, S. J.; Lv, F. T.; Gao, L. N.; Ding, L. P.; Fang, Y. *Langmuir* **2007**, *23*, 1584–1590.
(27) Leroy-Lhez, S.; Fages, F. *Eur. J. Org. Chem.* **2005**, 2684–2688.
(28) Swager, T. M.; Gil, C. J.; Wrighton, M. S. *J. Phys. Chem.* **1995**, *99*, 4886–4893.
(29) Kurth, D. G.; Bein, T. *Langmuir* **1993**, *9*, 2965–2973.
(30) (a) Mikroyannidis, J. A. *Synth. Met.* **2005**, *155*, 125–129. (b) Farcas, A.; Jarroux, N.; Ghosh, I.; Guegan, P.; Nau, W. M.; Harabagiu, V. *Macromol. Chem. Phys.* **2009**, *210*, 1440–1449. (c) Zhao, Z. J.; Xu, X. J.; Jiang, Z. T.; Lu, P.; Yu, G.; Liu, Y. Q. *J. Org. Chem.* **2007**, *72*, 8345–8353. (d) Ohshita, J.; Yoshimoto, K.; Tada, Y.; Harima, Y.; Kunai, A.; Kunugi, Y.; Yamashita, K. *J. Organomet. Chem.* **2003**, *678*, 33–38.
(31) Lakowicz, J. R. *Principles of Fluosescence Spectroscopy*, 3rd ed.; Springer-Verlag: Berlin, 2006.
(32) Marcus, R. A. *Rev. Mod. Phys.* **1993**, *65*, 599–610.
(33) (a) Hayase, S.; Hrovat, D. A.; Borden, W. T. *J. Am. Chem. Soc.* **2004**, *126*, 10028–10034. (b) Cai, Z. L.; Crossley, M. J.; Reimers, J. R.; Kobayashi, R.; Amos, R. D. *J. Phys. Chem. B* **2006**, *110*, 15624–15632. (c) Luo, Y. J.; Zhang, C. X.; She, Y. B.; Zhong, R. G.; Wei, P. *React. Kinet. Mech. Catal.* **2010**, *101*, 291–300.
(34) Frisch, M. J.; Trucks, G. W.; Schlegel, H. B.; Scuseria, G. E.; Robb, M. A.; Cheeseman, J. R.; Scalmani, G.; Barone, V.; Mennucci, B.; Petersson, G. A.; Nakatsuji, H.; Caricato, M.; Li, X.; Hratchian, H. P.; zmaylov, A. F. B., J.; Zheng, G.; Sonnenberg, J. L.; Hada, M. E., M.; Toyota, K.; Fukuda, R.; Hasegawa, J.; Ishida, M.; Nakajima, T.; Honda, Y.; Kitao, O.; Nakai, H.; Vreven, T.; Montgomery, J., J. A.; Peralta, J. E.; Ogliaro, F.; Bearpark, M.; Heyd, J. J.; Brothers, E.; Kudin, K. N.; Staroverov, V. N.; Kobayashi, R.; Normand, J.; Raghavachari, K.; Rendell, A.; Burant, J. C.; Iyengar, S. S.; Tomasi, J.; Cossi, M.; Rega, N.; Millam, N. J.; Klene, M.; Knox, J. E.; Cross, J. B.; Bakken, V.; Adamo, C.; Jaramillo, J.; Gomperts, R.; Stratmann, R. E.; Yazyev, O.; Austin, A. J.; Cammi, R.; Pomelli, C.; Ochterski, J. W.; Martin, R. L.; Morokuma, K.; Zakrzewski, V. G.; Voth, G. A.; Salvador, P.; Dannenberg, J. J.; Dapprich, S.; Daniels, A. D.; Farkas, Ö.; Foresman, J. B.; Ortiz, J. V.; Cioslowski, J.; Fox, D. J. *Guassian 09*; Guassian Inc.: Wallingford, CT, 2009.
(35) Lemaur, V.; Steel, M.; Beljonne, D.; Bredas, J. L.; Cornil, J. *J. Am. Chem. Soc.* **2005**, *127*, 6077–6086.
(36) Du, H. Y.; He, G.; Liu, T. H.; Ding, L. P.; Fang, Y. *J. Photochem. Photobiol., A* **2010**, *217*, 356–362.
(37) Kwak, G.; Lee, W.-E.; Jeong, H.; Sakaguchi, T.; Fujiki, M. *Macromolecules* **2009**, *42*, 20–24.